ACADEMIC PRESS

Available online at www.sciencedirect.com
SCIENCE DIRECT®

Journal of Sound and Vibration 263 (2003) 1055–1069

JOURNAL OF SOUND AND VIBRATION

www.elsevier.com/locate/jsvi

Multiwave non-linear couplings in elastic structures. Part II: two-dimensional example

D.A. Kovriguine[a], G.A. Maugin[b,*], A.I. Potapov[a]

[a] *Mechanical Engineering Institute, Russian Academy of Science, Nizhny-Novgorod, Russia*
[b] *Laboratoire de Modélisation en Mécanique, Université Pierre et Marie Curie, UMR 7607 CNRS, Case 162, 4 place Jussieu, 75252 Paris, Cedex 05, France*

Accepted 4 February 2003

Abstract

The non-linear resonance coupling in a thin plate in the Kirchhoff-Love approximation is selected as a two-dimensional example of mechanical systems exhibiting a rich range of resonant wave-like phenomena. This is originally examined by use of Whitham's average-Lagrangian method. In particular, the existence of three basic resonant triads between longitudinal, shear and bending modes is shown. Some of these necessarily enter cascade wave processes related to the instability of some of the mode components of the triad under small perturbations. A short comparison with Kolmogorov's cascades of turbulence is given.

1. Introduction

The phenomenon of non-linear resonance coupling classically occurs in physical systems that are governed by distinct modes of propagation; these may be of similar physical nature—e.g., various mechanical modes—or they may be of totally different nature—say, mechanical and magnetic or electric—as is often the case. In any case the two basic ingredients needed are (i) the existence of *multimodes* in the physical system and (ii) the *dispersion* of these modes in the linearized case. Such physical situations have received the attention of applied mathematicians and wave specialists in various fields of physics and engineering science, e.g., in non-linear optics and radiophysics (cf. [1,2]), in fluid dynamics (cf. [3]), and in elastic crystals with a microstructure (cf. [4,5]). In the case of elastic crystals the multimodes are due to a coupling of classical elastic d.o.f. with the kinematics of an internal structure—a rigid

*Corresponding author. Tel.: +33-144275312; fax: +33-144275259.
E-mail address: gam@ccr.jussieu.fr (G.A. Maugin).

doi:10.1016/S0022-460X(03)00274-8

mechanical one such as in micropolar media and liquid crystals, a magnetic one such as in ferromagnets (coupling between phonons and magnons), and an electric one in ferroelectric bodies (electroelastic couplings).

In Part 1 [6], one-dimensional (in space) non-linear motions involving 2-d.o.f. in elastic engineering structures were considered. In the present Part 2, the attention is focused on the non-linear wave couplings in an exemplary two-dimensional (in space) example, the one provided by non-linear waves in a thin elastic plate. The latter is modelled as a Kirchhoff–Love thin-walled plate. The corresponding governing equations of the second order in the non-linearity parameter are derived in Section 2. Linear modes of the longitudinal, shear and bending types are introduced in Section 3. This allows one to define the interactions between the dispersion manifolds with the possibilities of group- and phase-velocity matching. Weakly non-linear waves are studied starting in Section 4 on the basis of Whitham's average-Lagrangian theory [7,8], also Ref. [4, Appendix A.5], and Ref. [9, Chapter 4]. This is seldom exploited in solid mechanics, notable exceptions being in Maugin and Hadouaj [10] and the thesis of one of the authors [11]. This is the main originality of this contribution. For lack of space only some of the possibilities of non-linear resonance couplings are exhibited. A complete study is given in a long unpublished report [12]. The study reveals that among the possible resonant triads that can be identified exhibiting phase matching and the appropriate non-linear coupling, only *three* provide the building blocks of further wave constructs. Indeed, a brief study of the evolution of resonant triads shows that some of these are isolated while others have unstable components that inevitably interact with other triads. This yields the concept of *cascade wave processes* following along ideas of Richardson [13] and Landau [14]. This is briefly discussed by way of conclusion. The necessarily sketchy nature of the paper is emphasized as long cumbersome formulas of repetitive form are to be found in the already mentioned long memoir [12].

2. Basic equations

The model considered is one of a thin-walled plate in the long-wave limit on the basis of the theory of thin-walled shells. That is, h being the thickness and λ a typical wavelength, then $h/\lambda \ll 1$ (e.g., 0.1). Let $u_{(x)}, u_{(y)}, u_{(z)}$ be the longitudinal and transverse displacement components in the plate and $u(x,y,t), v(x,y,t), w(x,y,t)$ the longitudinal and transverse components of the displacement of the middle surface of the plate at $z=0$. In the Love–Kirchhoff approximation one has the truncated representations

$$u_{(x)} = u(x,y,t) - zw_x(x,y,t),\ u_{(y)} = v(x,y,t) - zw_y(x,y,t),$$
$$u_{(z)} = w(x,y,t), \tag{1}$$

where subscripts now denote partial spatial differentiation and t is the time. The related deformation components are

$$\varepsilon_{xx} = u_x - zw_{xx} + \tfrac{1}{2}u_x^2,\ \varepsilon_{yy} = v_y - zw_{yy} + \tfrac{1}{2}v_y^2,$$
$$\varepsilon_{xy} = \tfrac{1}{2}(u_y + v_x - 2zw_{xy} + w_xw_y). \tag{2}$$

In this approximation, with a material obeying Hooke's law in the adiabatic regime, the densities of kinetic energy and (potential) elastic energy per unit surface of the plate are given by

$$K = \tfrac{1}{2}\rho h(u_t^2 + v_t^2 + w_t^2), \tag{3}$$

$$\Pi = \frac{Eh}{2(1-\nu^2)}\int_{-h/2}^{h/2}\left[\varepsilon_{xx}^2 + \varepsilon_{yy}^2 + 2\nu\varepsilon_{xx}\varepsilon_{yy} + 2(1-\nu)\varepsilon_{xy}^2\right], \tag{4}$$

where E, ν and ρ denote Young's modulus, the Poisson ratio, and the mass density, respectively. With λ a typical wavelength and $c = \sqrt{E/(1-\nu^2)\rho}$, denoting a typical linear elastic wave speed, a non-dimensionalization is achieved with primed quantities defined by

$$u = \lambda u', \ldots, \quad x = \lambda x', \ldots, \quad t = (\lambda/c)t' \tag{5}$$

using now the primed quantities but then droping the primes to lighten the notation, the Lagrangian density $L = K - \Pi$ per unit area of the plate is given by

$$\begin{aligned} 2L = {} & \left[u_t^2 + v_t^2 + w_t^2\right] - \left[u_x^2 + \alpha^2(w_{xx}^2 + w_{yy}^2) + v_y^2\right] \\ & - 2\nu\left[v_y u_x + \alpha^2 w_{ww} w_{yy}\right] - \frac{(1-\nu)}{2}\left[u_y^2 + v_x^2 + 4\alpha^2 w_{xy}^2\right] \\ & - \mu\left[v_y(w_y^2 + \nu w_x^2) + u_x(w_x^2 + \nu w_y^2) + (1-\nu)(u_y + v_x)w_x w_y\right] \\ & - \frac{\mu^2}{4}(w_x^2 + w_y^2) + 0(\mu^3), \end{aligned} \tag{6}$$

where $\alpha = h/\sqrt{12}\lambda$ is a non-dimensional radius of inertia and

$$\mu = \max\sqrt{(u'^2 + v'^2 + w'^2)/\lambda} \tag{7}$$

is a *small parameter* that characterizes the *non-linearity* in the present problem. The Euler–Lagrange variational equations deduced from (6) read:

$$u_{tt} - u_{xx} - \frac{(1-\nu)}{2}u_{yy} - \frac{(1+\nu)}{2}v_{xy} = \frac{\mu}{2}\partial_x(w_x^2 + \nu w_y^2) + \mu\frac{(1-\nu)}{2}\partial_y(w_x w_y), \tag{8a}$$

$$v_{tt} - v_{yy} - \frac{(1-\nu)}{2}v_{xx} - \frac{(1+\nu)}{2}u_{xy} = \frac{\mu}{2}\partial_y(w_y^2 + \nu w_x^2) + \mu\frac{(1-\nu)}{2}\partial_x(w_y w_x) \tag{8b}$$

and

$$\begin{aligned} w_{tt} + \alpha^2\nabla^4 w = {} & \mu\partial_x\left[w_x(u_x + \nu v_y) + \frac{1-\nu}{2}w_y(u_y + v_x)\right] \\ & + \mu\partial_y\left[w_y(v_y + \nu u_x) + \frac{1-\nu}{2}w_x(u_y + v_x)\right] \\ & + \frac{\mu^2}{2}\partial_x\left[w_x(w_x^2 + w_y^2)\right] + \frac{\mu^2}{2}\partial_y\left[w_y(w_x^2 + w_y^2)\right], \end{aligned} \tag{8c}$$

where all the non-linear terms are in the right hand sides and $\nabla^4 = \partial_x^4 + 2\partial_x^2\partial_y^2 + \partial_y^4$.

3. Dispersion of linear waves

On setting $\mu = 0$, the following linear wave system can be deduced from Eq. (8) :

$$u_{tt} - u_{xx} - \frac{(1-\nu)}{2}u_{yy} - \frac{(1+\nu)}{2}v_{xy} = 0, \tag{9a}$$

$$v_{tt} - v_{yy} - \frac{(1-\nu)}{2}v_{xx} - \frac{(1+\nu)}{2}u_{xy} = 0, \tag{9b}$$

$$w_{tt} + \alpha^2\nabla^4 w = 0. \tag{9c}$$

The dispersion branches $\omega_j = \bar{\omega}_j(\mathbf{k}), j = l, s, b;\ \mathbf{k} = \{k_x, k_y\}$, of this system are given by

- highly dispersive bending waves:

$$\omega_b = \alpha|\mathbf{k}|^2, \tag{10}$$

- dispersionless shear waves:

$$\omega_s = \sqrt{(1-\nu)/2}|\mathbf{k}|, \tag{11}$$

- dispersionless longitudinal waves:

$$\omega_l = |\mathbf{k}|. \tag{12}$$

Further $a_j(\mathbf{k})$ are called complex constant amplitudes, $\phi_j(\omega_j, \mathbf{k}) = \omega_j t - \mathbf{k}.\mathbf{x}$, the phases, and $\Psi_l(\mathbf{k}) = \{\psi_l^u(\mathbf{k}), \psi_l^v(\mathbf{k})\}$ and $\Psi_s(\mathbf{k}) = \{\psi_s^u(\mathbf{k}), \psi_s^v(\mathbf{k})\}$ the so-called polarization vectors, which define the mode shape on the plane of the plate. One therefore has

$$\psi_l^v(\mathbf{k}) = p_l(\mathbf{k})\ \psi_l^u(\mathbf{k}), \quad \psi_s^v(\mathbf{k}) = p_s(\mathbf{k})\psi_s^u(\mathbf{k}), \tag{13}$$

where the functions

$$p_l(\mathbf{k}) = k_x/k_y, \quad p_s(\mathbf{k}) = -k_y/k_x \tag{14}$$

are the interrelation coefficients satisfying the orthogonality condition: $p_l(\mathbf{k})p_s(\mathbf{k}) = -1$. In order to unify the notation an interrelation for bending waves is introduced formally, such that $p_b(\mathbf{k}) \equiv 0$.

It must be noted that there are two characteristic manifolds on the dispersion surface of bending waves (10). These manifolds are represented by closed curves, namely, the *group-velocity matching curve* such that

$$\omega_g^{(s)} = (1-\nu)/8\alpha, \quad \left|\mathbf{k}_g^{(s)}\right| = \sqrt{1-\nu}/2\sqrt{2}\alpha, \tag{15}$$

where the propagation velocity of shear waves coincides with that of bending waves, and the *phase-velocity matching curve*:

$$\omega_{ph}^{(s)} = (1-\nu)/2\alpha, \quad \left|\mathbf{k}_{ph}^{(s)}\right| = \sqrt{1-\nu}/\sqrt{2}\alpha, \tag{16}$$

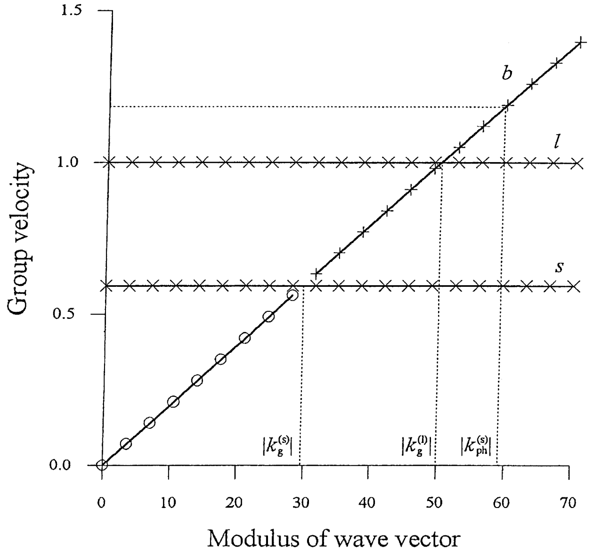

Fig. 1. Intersection of the dispersion surfaces by a plane passing through the axis of natural frequencies. Loci of this plane with the surfaces of the group- and phase-matchings are shown.

where the velocities of shear and bending waves are the same. These matching manifolds belong to two circles of different radii created as the intersection between the planes $\omega = \omega_g^{(s)}$ and $\omega = \omega_{ph}^{(s)}$ and the bending-wave dispersion surface given by Eq. (10) in the space of spectral parameters (see Fig. 1). In the subsequent non-linear analysis the range of wave vectors is limited by $|\mathbf{k}| < 1/2\alpha$ where the group velocity does not exceed the characteristic velocity of elastic waves.

The general linear-wave solution of system (9) is

$$\begin{aligned} u(x,t) &= \iint \mathrm{d}k_x \mathrm{d}k_y \left[a_l \psi_l^u \exp \mathrm{i}\phi_l + a_s \psi_s^u \exp \mathrm{i}\phi_s \right] + (\cdot)^*, \\ v(x,t) &= \iint \mathrm{d}k_x \mathrm{d}k_y \left[a_l p_l \psi_l^u \exp \mathrm{i}\phi_l + a_s p_s \psi_s^u \exp \mathrm{i}\phi_s \right] + (\cdot)^*, \\ w(x,t) &= \iint \mathrm{d}k_x \mathrm{d}k_y a_b \exp \mathrm{i}\phi_b + (\cdot)^*, \end{aligned} \tag{17}$$

where (.)* denotes the complex conjugate of the preceding term.

4. Weakly non-linear analysis: resonant triads

When the parameter μ is non-zero but still very small, the right hand sides in Eq. (8) stand for a weak non-linearity and they produce only small amplitude variations measured on the slow temporal scale $\tau = \mu t$ and slow spatial scales $\chi = \{\mu x; \mu y\}$. Any formal solution to Eq. (8) may be represented in the same form as in Eq. (17) but with amplitudes a_j that should now depend also upon the slowly varying spatio-temporal arguments τ and χ. When substituting from (17) modified in such a manner into the basic set of Eq. (8), there results a set of non-linear integro-differential equations that describe the spatio-temporal evolution of phases and amplitudes. In order to simplify the structure of this rather complicated system, one should try first to uncover those "primary" d.o.f. which define the general dynamical features of the system. Simultaneously, one should drop all "secondary" d.o.f. which will produce only small corrections to the spatio-temporal evolution. With a view to give a satisfactory mathematical sketch along this line of thought, one must investigate the so-called *resonant manifolds* along which the *phase matching* conditions hold true. Note that the presence of the resonant manifold in the space of natural frequencies and wave vectors is a necessary condition for the appearance of a non-linear resonant coupling between quasi-harmonics due to so-called *internal resonances*, while sufficient conditions are defined by the concrete form of the non-linearity under consideration. Here, in the simplest case the non-linear coupling of wave triads is expected in the investigated system because the lowest order non-linearity in the basic Eq. (8) is quadratic. The triple-wave phase matching conditions read

$$\mathbf{k}_1 = \mathbf{k}_2 + \mathbf{k}_3, \quad \omega_\alpha(\mathbf{k}_1) = \omega_\beta(\mathbf{k}_2) + \omega_\gamma(\mathbf{k}_3), \tag{18}$$

where the natural frequencies are numbered in the following order:

$$\omega_\alpha(\mathbf{k}_1) \geqslant \omega_\beta(\mathbf{k}_2) \geqslant \omega_\gamma(\mathbf{k}_3), \tag{19}$$

and the indices α, β and γ can be arbitrary ones from the set $\{l, s, b\}$ which corresponds to the longitudinal, shear and bending modes, respectively. When both the phase matching conditions and an appropriate type of non-linearity hold true, then there arise triple-wave resonant ensembles that we call *resonant triads*. Given the richness of the present dynamical system, there formally exist

$$\sum_{n=0}^{3} \frac{3!}{n!(3-n)!} \sum_{m=0}^{3-n} \frac{(3-n)!}{m!(3-n-m)!} = 27 \tag{20}$$

potential types of phase matching conditions (18), since the role of high- and low-frequency modes inside any arbitrary triad may be played by waves of any type. The question naturally arises of selecting only those physical matching conditions that make sense, since the others may simply result from some geometrical formalism. This can be answered by examining the concrete structure of the present non-linearity. This will simplify the problem without loss of general dynamical properties of the system. To do so Whitham's method of the average Lagrangian is first used and then the most representative resonant triads selected.

4.1. Average Lagrangian

We write

$$\bar{L}(\tau, \chi) = \langle L(\mathbf{x}, t, \tau, \chi) \rangle = \frac{1}{(2\pi)^3} \int_0^{2\pi} \int_0^{2\pi} \int_0^{2\pi} L \, \mathrm{d}\phi_l \, \mathrm{d}\phi_s \, \mathrm{d}\phi_b, \tag{21}$$

where $\phi_j = \omega_j t - \mathbf{k}.\mathbf{x}$. Following Whitham [7,9], the average Lagrangian is expanded in a power series of μ, i.e., $\bar{L}(\tau, \chi) = \bar{L}_2 + \mu \bar{L}_3 + 0(\mu^2)$. The vanishing of the first term is none other than the dispersion relations written in explicit form as $D_\alpha = \omega_\alpha^2 - \omega_\alpha^2(\mathbf{k}) \equiv 0$, $\alpha = s, l, b$. At the first order in μ, one has Euler–Lagrange equations derived from $\bar{L}_3$ that describe the slow spatial-temporal variations of the complex amplitudes in the form

$$\frac{\partial \bar{L}_3}{\partial a_n{}^*} - \frac{\mathrm{d}}{\mathrm{d}\tau}\frac{\partial \bar{L}_3}{\partial(\mathrm{d}a_n{}^*/\mathrm{d}\tau)} - \boldsymbol{\nabla}_\chi \frac{\partial \bar{L}_3}{\partial(\boldsymbol{\nabla}_\chi a_n{}^*)} = 0, \tag{22}$$

where the asterisk again denotes complex conjugacy. In the simplest case where the phase matching conditions (18) for a single triad of quasi-harmonic waves hold good, the average Lagrangian has the following structure:

$$\begin{aligned}\bar{L}_3 = & -\mathrm{i}\varpi_\alpha(\mathbf{k}_1)\left(a_\alpha{}^*(\mathbf{k}_1)\frac{\partial a_\alpha(\mathbf{k}_1)}{\partial\tau} - (\cdot)^*\right)\\ & -\mathrm{i}\varpi_\beta(\mathbf{k}_2)\left(a_\beta{}^*(\mathbf{k}_2)\frac{\partial a_\beta(\mathbf{k}_2)}{\partial\tau} - (\cdot)^*\right)\\ & -\mathrm{i}\varpi_\gamma(\mathbf{k}_3)\left(a_\gamma{}^*(\mathbf{k}_3)\frac{\partial a_\gamma(\mathbf{k}_3)}{\partial\tau} - (\cdot)^*\right)\\ & -\mathrm{i}\mathbf{v}_\alpha(\mathbf{k}_1)\varpi_\alpha(\mathbf{k}_1)\left[a_\alpha{}^*(\mathbf{k}_1)\boldsymbol{\nabla}_\chi a_\alpha(\mathbf{k}_1) - (\cdot)^*\right]\\ & -\mathrm{i}\mathbf{v}_\beta(\mathbf{k}_2)\varpi_\beta(\mathbf{k}_2)\left[a_\beta{}^*(\mathbf{k}_2)\boldsymbol{\nabla}_\chi a_\beta(\mathbf{k}_2) - (\cdot)^*\right]\\ & -\mathrm{i}\mathbf{v}_\gamma(\mathbf{k}_3)\varpi_\gamma(\mathbf{k}_3)\left[a_\gamma{}^*(\mathbf{k}_3)\boldsymbol{\nabla}_\chi a_\gamma(\mathbf{k}_3) - (\cdot)^*\right]\\ & -\mathrm{i}\beta_{ijk}(\mathbf{k}_1,\mathbf{k}_2,\mathbf{k}_3)\left[a_\alpha{}^*(\mathbf{k}_1)a_\beta(\mathbf{k}_2)a_\gamma(\mathbf{k}_3) - (\cdot)^*\right],\end{aligned} \tag{23}$$

where $\mathbf{v}_\alpha(\mathbf{k}) = \{v_{\alpha x}(\mathbf{k}), v_{\alpha y}(\mathbf{k})\}$ are the group velocities of the waves

$$\varpi_\alpha(\mathbf{k}) = \omega_\alpha(\mathbf{k})[1 + p_\alpha(\mathbf{k})] \tag{24}$$

and β_{ijk} are functions of the wave vectors which characterize the resonance coupling inside the selected triad (i,j,k). Eq. (22) then form a set of hyperbolic partial differential equations of the form

$$\frac{\partial a_\alpha(\mathbf{k}_1)}{\partial\tau} + \mathbf{v}_\alpha(\mathbf{k}_1)\boldsymbol{\nabla}_\chi a_\alpha(\mathbf{k}_1) = \frac{\beta ijk}{\varpi_\alpha(\mathbf{k}_1)}\frac{\partial U}{\partial a_\alpha{}^*(\mathbf{k}_1)} \tag{25}$$

with similar equations for β and γ with the appropriate dependence on $\mathbf{k}_2$ and $\mathbf{k}_3$. The potential U given by

$$U = a_\alpha{}^* a_\beta a_\gamma - a_\alpha a_\beta{}^* a_\gamma{}^* \tag{26}$$

is the average potential of the triple-wave resonant coupling (compare to Kovriguine et al. [6]).

4.2. Three types of resonant non-linear triads in the plate

Consider the propagation of a small perturbed quasi-harmonic wave in order to evaluate its stability with respect to the other waves combined into a resonant triad. Let this wave play the role of the high-frequency mode $(\omega_1, \mathbf{k}_1)$ in the triad (18), (19). A pair of its low-frequency satellites is associated with two points $(\omega_2, \mathbf{k}_2)$ and $(\omega_3, \mathbf{k}_3)$ at the intersections of the dispersion surfaces defined by Eqs. (10) and (12), provided $|\mathbf{k}| < 1/2\alpha$ (see end of Section 3). These intersections result from a permanent translation of one of the dispersion surfaces with respect to the others, as the origin of any surface moves on the surface of the other. These loci define the parameters of resonant triads in the spectral space $(\omega, \mathbf{k})$ in agreement with the matching conditions (18). In order to define the possible types of actually realizable triads, we call T_{lbb}, T_{sbb}, T_{bsb} triads where indices identify the modal state of the triad (obviously, l for longitudinal mode, s for shear mode, b for bending mode). These indices are here numbered so as to respect the order defined by the matching conditions (18).

First type: To the primary high-frequency *longitudinal* wave, there always correspond two secondary low-frequency bending waves on the resonant manifold belonging to the dispersion surface of bending waves and defined by the expression: $|\mathbf{k}_1| = \alpha(|\mathbf{k}_2|^2+|\mathbf{k}_3|^2)$, i.e., the T_{lbb} triad (cf. Fig. 2).

Second type: If the shear wave is the high-frequency mode, then there exist two secondary low-frequency bending waves on the resonant manifold belonging to the dispersion surface (10) and defined by the expression $\alpha(|\mathbf{k}_2|^2+|\mathbf{k}_3|^2) = \sqrt{(1-\nu)/2}|\mathbf{k}_1|$, hence the T_{sbb} triad (cf. Fig. 3).

Third type: If the primary wave is a bending mode while the secondary waves are one bending wave and one shear wave, we have a third type of resonant triad. This corresponds to a resonant manifold defined as the intersection of the surfaces $\omega = \alpha|\mathbf{k}|^2$ and $\omega - \omega_1 = \sqrt{(1-\nu)/2}|\mathbf{k}| - |\mathbf{k}_1|$, where $\alpha(|\mathbf{k}_1|^2-|\mathbf{k}_2|^2) = \sqrt{(1-\nu)/2}|\mathbf{k}_3|$. This defines a T_{bsb} triad (cf. Fig. 4).

Remarkably enough the three types of triads just defined are physical ones for which both the phase matching conditions and the appropriate type of non-linearity in the governing equations hold true. As a matter of fact, any resonant triad in the plate consists of a pair of bending waves and one longitudinal or shear wave. The reason for this is that in the initial Lagrangian there are no such terms as $v_y u_y v_x$ or u_y^3, which would create other hypothetical types of triads. This, in turn, means that there are no other types of triple-resonant interactions within the present mathematical model of a plate than the three already identified types.

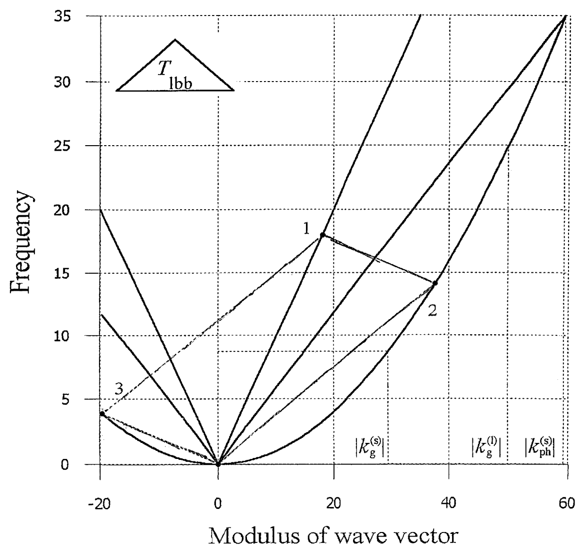

Fig. 2. Scheme of the spectral state of T_{lbb}-type resonant triads (on a plane passing through the axis of natural frequencies.

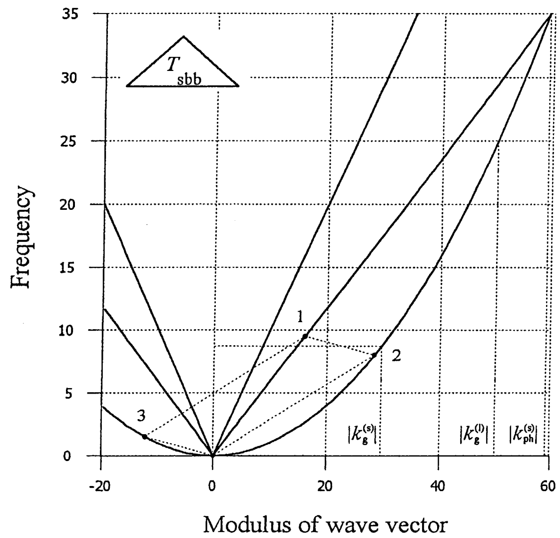

Fig. 3. Scheme of the spectral state of T_{sbb}-type resonant triads.

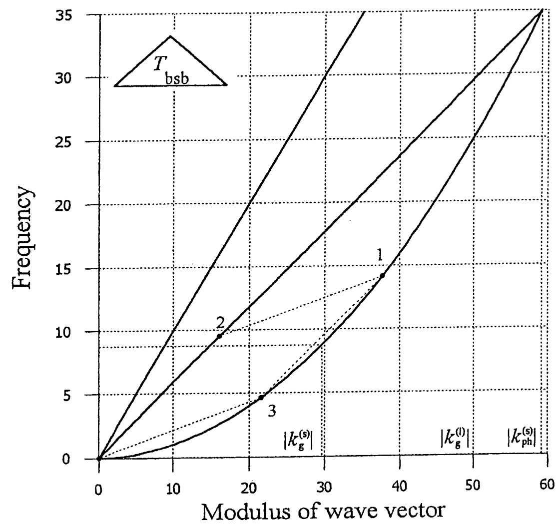

Fig. 4. Scheme of the spectral state of T_{bsb}-type resonant triads.

5. Evolution of resonant triads

Truncated equations governing the evolution of triple-wave resonant ensembles may now be derived. Only the case of the T_{lbb}-triad will be examined, the reader being referred to a long memoir for the parallel treatment of the other two cases [12]. For this selected triad the solution of

Eq. (8) is sought in the form

$$
\begin{aligned}
u(\mathbf{x},t) &= A_1(\chi,\eta,\tau)\exp \mathrm{i}\Phi_1 + (\cdot)^*,\\
\mathrm{v}(\mathbf{x},t) &= B_1(\chi,\eta,\tau)\exp \mathrm{i}\Phi_1 + (\cdot)^*,\\
w(\mathbf{x},t) &= A_2(\chi,\eta,\tau)\exp \mathrm{i}\Phi_2 + A_3(\chi,\eta,\tau)\exp \mathrm{i}\Phi_3 + (\cdot)^*,
\end{aligned}
\tag{27}
$$

where $\Phi_i = \omega_i t - \mathbf{k}_i.\mathbf{x}$, and the complex amplitudes of planar quasi-harmonic waves slowly vary on the spatio-temporal scales $\chi = \mu x, \eta = \mu \mathrm{y}, \tau = \mu t$. The average Lagrangian characterizing the evolution of the triad (27) reads

$$
\begin{aligned}
\bar{L}_3 = &- \mathrm{i}\omega_1\left(1+p_l^2(k_1)\right)\left(\frac{\partial A_1}{\partial \tau}A_1^* - \frac{\partial A_1^*}{\partial \tau}A_1\right) - \mathrm{i}\sum_{n=2,3}\omega_n\left(\frac{\partial A_n}{\partial \tau}A_n^* - \frac{\partial A_n^*}{\partial \tau}A_n\right)\\
&- \mathrm{i}k_{1x}\left(1+p_l^2(k_1)\right)\left(\frac{\partial A_1}{\partial \chi}A_1^* - \frac{\partial A_1^*}{\partial \chi}A_1\right) - \mathrm{i}k_{1y}\left(1+p_l^2(k_1)\right)\left(\frac{\partial A_1}{\partial \eta}A_1^* - \frac{\partial A_1^*}{\partial \eta}A_1\right)\\
&- 2\mathrm{i}\alpha^2\sum_{n=2,3}k_{nx}|k_n|^2\left(\frac{\partial A_n}{\partial \chi}A_n^* - \frac{\partial A_n^*}{\partial \chi}A_n\right) - 2\mathrm{i}\alpha^2\sum_{n=2,3}k_{ny}|k_n|^2\left(\frac{\partial A_n}{\partial \eta}A_n^* - \frac{\partial A_n^*}{\partial \eta}A_n\right)\\
&- \mathrm{i}\beta_{lbb}(A_1A_1^*A_1^* - A_1^*A_2A_3),
\end{aligned}
$$

where $p_l(k_1 = A_1/B_1)$. The amplitude governing equations are obtained in the form

$$
\begin{aligned}
\frac{\partial A_1}{\partial \tau} + v_{1x}\frac{\partial A_1}{\partial \chi} + v_{1y}\frac{\partial A_1}{\partial \eta} &= \beta_{lbb}\varpi_1^{-1}A_2A_3,\\
\frac{\partial A_2}{\partial \tau} + v_{2x}\frac{\partial A_2}{\partial \chi} + v_{2y}\frac{\partial A_2}{\partial \eta} &= \beta_{lbb}\varpi_2^{-1}A_1A_3^*,\\
\frac{\partial A_3}{\partial \tau} + v_{3x}\frac{\partial A_3}{\partial \chi} + v_{3y}\frac{\partial A_3}{\partial \eta} &= \beta_{lbb}\varpi_3^{-1}A_1A_2^*.
\end{aligned}
\tag{28}
$$

Here

$$
\mathbf{v}_1(\mathbf{k}_1) = \left\{\frac{k_{1x}}{|\mathbf{k}_1|}, \frac{k_{1y}}{|\mathbf{k}_1|}\right\}, \quad \mathbf{v}_\alpha(\mathbf{k}_\alpha) = \left\{2\alpha k_{\alpha x}, 2\alpha \mathrm{k}_{\alpha \mathrm{y}}\right\}
$$

are the group velocities of the longitudinal waves and of the bending waves , respectively. The non-linear-coupling coefficient β_{lbb} is given by

$$
\begin{aligned}
\beta_{lbb} = &\, p_l(\mathbf{k}_1)k_{1y}\left(k_{2y}k_{3y} + vk_{2x}k_{3x}\right) + k_{1x}\left(k_{2x}k_{3x} + vk_{2y}k_{3y}\right)\\
&+ \left(\frac{1-v}{2}\right)\left(k_{1y} + p_l(\mathbf{k}_1)k_{1x}\right)\left(k_{2x}k_{3y} + vk_{2y}k_{3x}\right).
\end{aligned}
\tag{29}
$$

Analyses of the same type hold good for the other two-resonance triad T_{sbb} and T_{bsb} with different expressions for the coefficient (29)—interchange of indices in the appropriate manner. The relevant expressions are to be found in Ref. [12]. These results, through first integrals of systems of the type (28), globally allow one to discuss the stability of modes of propagation. In particular, such a discussion shows why some resonant triads are isolated and why others cannot be isolated. The following results are reached:

(i) Intense high-frequency longitudinal or shear waves are *unstable* with respect to small perturbations as a result of the break-up instability within the T_{lbb} or T_{sbb} triads.

(ii) Intense bending waves, the group velocity of which is less than the phase velocity of shear waves

$$\left(|\mathbf{\Delta_k}\omega| < \sqrt{(1-\nu)/2}\right) \tag{30}$$

are *stable* with respect to small perturbations, since there is no break-up instability in the T_{bsb}-type of triads.

(iii) If the group velocity of bending waves exceeds the group velocity of shear waves (Eq. (30) with reverse inequality sign), then such waves are *unstable* due to the T_{bsb} type of resonance coupling.

However, there is an essential difference in the dynamical behavior of the T_{lbb}, T_{sbb} triads, on the one hand, and the T_{bsb} triads on the other hand, which is revealed by their stability properties against a broad class of initial perturbations. Inside the range of group velocities (30), the T_{lbb} and T_{sbb} types of resonant triads are *isolating resonant ensembles* consisting of triplets of waves which conserve the total energy of triads, since the waves entering these ensembles do not interact with other resonant ensembles or other waves, at least within the present first order approximation analysis. In other words such isolating triads are stable with respect to small perturbations over any mode which makes up the triad. The existence domain of the T_{bsb}-type triads covers the range of group velocities of high-frequency bending waves (inequality (30) with reverse sign). Any intense bending wave with group velocity inside this range is disintegrated into two secondary waves under small perturbation. One of these secondary waves is a stable bending mode with group velocity inside the range (30), while the other secondary wave is an unstable shear wave which can be the breaking-up component with a T_{sbb}-type triad. This means that the T_{bsb}-type triad cannot be an *isolating* wave ensemble, since its secondary shear mode is always unstable against small perturbations. This leads us to the necessary consideration of the non-linear coupling between several resonant triads that are examined succinctly by way of conclusion.

6. Non-linear coupling between triads

One can see that any non-isolating resonant triad can be effectively coupled with other triads of other types and spectral states. To formulate the problem of the multi-wave non-linear coupling between triads, a structural scheme of modal interactions represented by a set of non-linearly coupled triads of different types and spectral scales ought to be investigated. Following pioneering works of Richardson [13] and Landau [14], this can be achieved based on the scenario of *cascade wave processes*. For instance, let the mid-frequency bending mode inside some T^1_{sbb}-type triad play at the same time the role of the unstable high-frequency mode entering the adjacent T^2_{bsb}-type triad occupied by a lower spectral tier. In turn, the mid-frequency shear mode entering this T^2_{sbb}-type triad loses its stable properties inside another T^3_{sbb}-type triad on the lower sale, etc. Note that in this cascade there is always some definite triad that occupies the lowest tier, say T^N_{sbb}, naturally called the ‘‘terminating ‘‘ triad which finishes the development of the triad-cell chain, since this triad appears as an isolating resonant ensemble, in which the secondary modes cannot break up. This is schematized in Fig. 5. Therefore, the total number of the T_{sbb} and T_{bsb}-type triad pairs in the plate is always limited. It should in fact be noted that the T_{lbb}-type triads cannot be structural

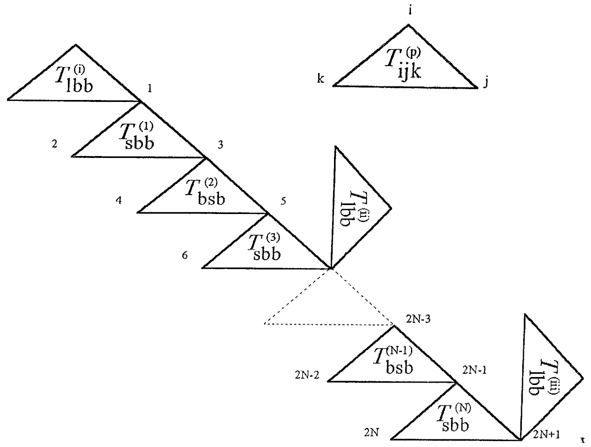

Fig. 5. Scheme of the resonant coupling of T_{lbb}-type triad with the resonant chain consisting of pairs of adjacent T_{sbb}- and T_{bsb}-type triads. Each triangle T^{p}_{ijk} denotes a triad cell, where p is the number of the triad tier, index i corresponds to the high-frequency mode of the given triad trier, index j denotes the mid-frequency mode, and k refers to the low-frequency mode.

elements of cascade processes developing the triad-cell chains in the elastic plate (Fig. 5). A complete analytical study would require establishing the evolution equations of triad-cell chains. This can be achieved within Lagrangian and Hamiltonian approaches related to the average since the present system does not contain any dissipation. The corresponding Euler–Lagrange equations reduce to ordinary differential equations for the amplitudes in the case of spatially uniform processes. Conservation laws and global integrals of the motion can be obtained as the law of partition of energy between waves and Manley–Rowe relations, respectively (compare to Part I of the present work [6]). For instance, for an arbitrary N (Fig. 5), one obtains $(N+1)$ integrals of the motion in the form of Manley–Rowe relations (compare to Eq. (15) in Part I)

$$\begin{gathered}\frac{E_1}{\omega_1}+\frac{E_2}{\omega_2}=\text{const.},\\ \frac{E_{2n}}{\omega_{2n}}-\frac{E_{2n+2}}{\omega_{2n+2}}-\frac{E_{2n-1}}{\omega_{2n-1}}=\text{const.},\quad n=(1,..,N-1),\\ \frac{E_{2N}}{\omega_{2N}}-\frac{E_{2N+1}}{\omega_{2N+1}}=\text{const.}\end{gathered}\tag{31}$$

and the finite triad-cell chain conserves the total energy

$$\sum_{n=1}^{2N+1}E_n=\text{const.},\tag{32}$$

where the E_i's are energies and the ω_i's are frequencies. One must notice that the accompanying system of evolution equations grows rapidly in size with the number N. This system possesses $(N+1)$ evident integrals of motions (31), the order of the system is $(3N+1)$ (for $(2N+1)$ amplitudes and N generalized phases), and it cannot be solved analytically. Notice that N being given, there are $(N-1)$ common modes in a cascade; then the total number of non-linear coupled modes indeed is $[3N-(N-1)]=(2N+1)$. If mode #1 is an unstable high-frequency shear mode, modes #2N and $(2N+1)$ are the unstable (with respect to small perturbations) bending waves. In particular, if the modal amplitudes #1 and #2 approach zero, then the cascade beginning from the unstable bending wave #3 in the triad should appear. So, both cases (cascades beginning from the high frequency shear mode and bending mode) hold true. The number N is determined by the wave number of the initially perturbed quasi-harmonic wave mode and the type (shear or bending) of the primary unstable mode #1. As an example, consider such a mode for a *shear* wave in a plate with dispersion parameters $\alpha=0.01$ and $\nu=0.3$, and with wave vector modulus $|\mathbf{k}_0|=40$—see the related group velocities in Fig. 1. In this case $N=9$ coupled resonant triads, and a total of 19 modes enter the triad cell chain. The corresponding spectral parameters of this modal chain are given in Fig. 6. Initial conditions are selected such that all above referred to generalized phases are zero while all modes possess equal portion of energy $E_n=0.1/(2N+1)$, with the exception of the first mode such that $E_1=1$. After careful evaluation of the source (coupling) terms in the system of evolution equations (see the lengthy expressions in Ref. [12]), this allows one to study numerically the ensuing energy partition between individual modes via the relation for the time averaged energies $\langle E_n\rangle$ as functions of the wave number modulus $|\mathbf{k}|$ for a sufficient time interval (cf. Fig. 7). Power laws can be fitted to this relation for odd and even modes separately. This is very much like the power law spectra predicted by the Kolmogorov–Zakharov cascade hypothesis in classical and plasma turbulence (compare Refs. [15,16]). However, the present cascades must be contrasted to those of the Kolmogorov type. The

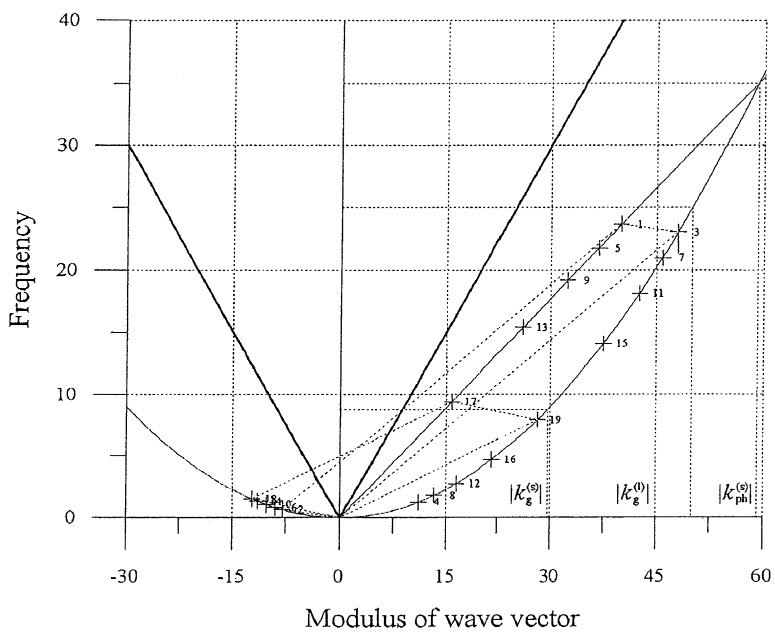

Fig. 6. Spectral parameters for a triad-cell chain $N=9$ with a weakly perturbed quasi-harmonic shear wave (19 modes are involved).

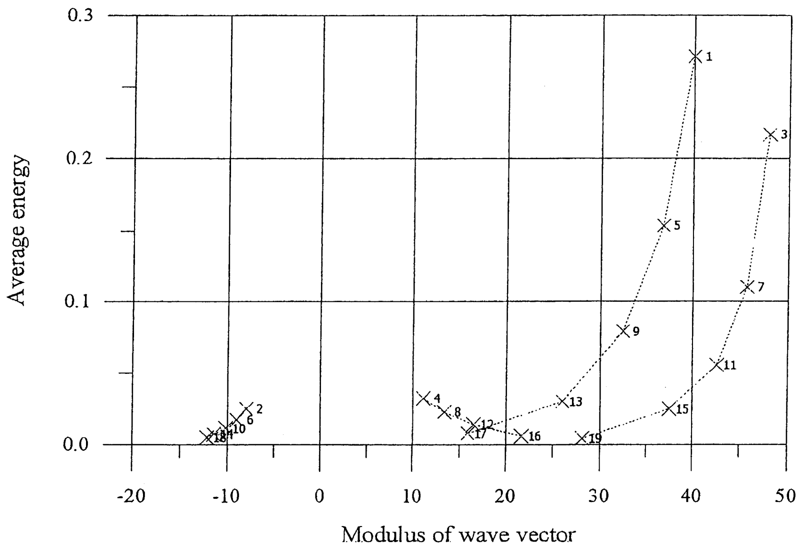

Fig. 7. Average energy partition for the triad-cell chain $N = 9$ corresponding to Fig. 6.

Kolmogorov [15] cascades refer to the so-called inertial interval between the large-scale pumping zone and the small-scale dissipation zone. In the triad-cells of the present mechanical system there are no source, pumping, and dissipation. Furthermore, the mechanical systems considered here possess a strong dispersion so that the mechanisms of temporal evolution are quite different from those in the Kolmogorov case. If it is true that in the latter case a large-scale vortex (small wave number) breaks up due to the generation of higher harmonics (by multiplying the main frequency), into a series of small vortices (large wave number) subject to strong molecular dissipation, in the present case the situation is opposite in the sense that the high-frequency waves breaks up producing, due to the dispersion and division of the main characteristic frequency, a series of low-frequency waves—which should have weak dissipation in real systems. Finally, the triad cells of the present work appear in the simplest case as discrete objects (quasi-particles), while the Kolmogorov cascade modelling in fluids refers to a continuum.

In conclusion it is emphasized that the study of the stationary patterns in resonant chains is of particular interest. The reason for this is that most transient wave patterns may be satisfactorily approximated by stationary ones at larger times and for large traveled distances. For these, the reader is referred to the computations given in a long memoir [12].

Acknowledgements

This research was conducted within the framework of the INTAS Program 96-2370 and 961-2370 between Paris and Nizhny-Novgorod. GAM benefits from a Max Planck Award for International Scientific Cooperation (2001–2005).

References

[1] A.P. Sukhorokov, Nonlinear Interactions of Waves in Optics and Radiophysics, Naouka, Moscow, 1988 (in Russian).

[2] D.F. Nelson, Electric, Optic and Acoustic Interactions in Dielectrics, Wiley-Interscience, New York, 1979.

[3] A.D.D. Craig, Wave Interactions and Fluid Flows, Cambridge University Press, Cambridge, UK, 1985.

[4] G.A. Maugin, Nonlinear Waves in Elastic Crystals, Oxford University Press, Oxford, UK, 1999.

[5] A.I. Potapov, A.S. Pavlov, G.A. Maugin, Nonlinear wave propagation in 1D crystals with complex structure, Wave Motion 29 (1998) 297–312.

[6] D.A. Kovriguine, G.A. Maugin, A.I. Potapov, Multiwave nonlinear couplings in elastic structures. Part 1: One-dimensional examples International Journal of Solid Structures (special issue dedicated to J.D. Achenbach) 39 (2002) 5571–5583.

[7] G.B. Whitham, Dispersive waves and variational principles, in: S. Leibovich, R. Seebass (Eds.), Nonlinear Waves, Cornell University Press, Ithaca, 1974, pp. 139–169.

[8] G.B. Whitham, Linear and Nonlinear Waves, Wiley-Interscience, New York, 1974.

[9] L.A. Ostrovsky, A.I. Potapov, Modulated Waves, Theory and Applications, Johns Hopkins University Press, Baltimore, 1999.

[10] G.A. Maugin, H. Hadouaj, Solitary surface transverse waves on an elastic substrate coated with a thin film solitary surface transverse waves on an elastic substrate coated with a thin film, Physics Review B 44 (1991) 1266–1280.

[11] D.A. Kovriguine, Nonlinear Resonant Interactions in Elastic Structural Members, Ph.D. Thesis, Nizhny-Novgorod University, Russia, 1992 (in Russian).

[12] D.A. Kovriguine, A.I. Potapov, G.A. Maugin, Multi-wave nonlinear couplings in elastic structures, Report INTAS Program 96-2370, Nizhny-Novgorod, Russia and Paris, France, 2001, 125pp.

[13] L.F. Richardson, Weather Prediction by Numerical Process, Cambridge University Press, Cambridge, UK, 1922.

[14] L.D. Landau, On the problem of turbulence, Soviet Physics Doklady 44(8) (1944) 311–314 (in Russian); reprinted in English translation in: L.D. Landau's Collected Papers, Oxford University Press, Oxford, 1965, pp. 387–391.

[15] A.N. Kolmogorov, On the local structure of turbulence in compressible fluids at very large Reynolds numbers, Doklady Akademii Nauk SSSR 85 (1941) 527 (in Russian).

[16] V.E. Zakharov, Kolmogorov spectra in weak turbulence problems, in: A.A. Galeev, R.N. Sudan (Eds.), Handbook of Plasma Physics, Vol. 2, North-Holland, Amsterdam, 1984.